NANO LETTERS

2006
Vol. 6, No. 5
953−957

Measurement of the Adhesion Force between Carbon Nanotubes and a Silicon Dioxide Substrate

Jed D. Whittaker,[†] Ethan D. Minot,[‡] David M. Tanenbaum,[§] Paul L. McEuen,[‡] and Robert C. Davis*,[†]

Department of Physics and Astronomy, Brigham Young University, Provo, Utah 84602, Laboratory of Atomic and Solid State Physics, Cornell University, Ithaca, New York 14853, and Department of Physics and Astronomy, Pomona College, Claremont, California 91711

Received January 4, 2006; Revised Manuscript Received February 24, 2006

ABSTRACT

Carbon nanotube adhesion force measurements were performed on single-walled nanotubes grown over lithographically defined trenches. An applied vertical force from an atomic force microscope (AFM), in force distance mode, caused the tubes to slip across the 250-nm-wide silicon dioxide trench tops at an axial tension of 8 nN. The nanotubes slipped at an axial tension of 10 nN after being selectively coated with a silicon dioxide layer.

Carbon nanotubes (CNT) are routinely grown on silicon and silicon dioxide surfaces for use in research applications such as AFM probe tips,[1−3] nanomechanical systems,[4,5] and transistor devices.[6] It is not quantitatively known how well adhered the tubes are to the surface, although several authors have demonstrated that this adhesion is significant.[7−9] CNT adhesion has been useful in making mechanically robust composites and fibers.[10,11]

We used a suspended nanotube geometry to study nanotube−oxide adhesion forces with an AFM. SWNTs were grown across trenches that were defined in silicon dioxide using e-beam lithography and dry etching. The trenches were 300−400 nm wide and 40−50 nm deep. The suspended tubes were then pushed toward the trench bottom until slip occurred along their axis, as shown schematically in Figure 1a and b. Figure 1c shows that slipping indeed occurs because a suspended nanotube section was pushed until it stuck to the trench bottom. An adjacent suspended section was then pushed until it stuck to the trench bottom, and the original section was released from its trench bottom (Figure 1d).

We investigated how much the slipping force depends on the geometry of the nanotube−oxide interface. This dependence was investigated by measuring slipping at different nanotube−oxide contact lengths and by measuring slipping of nanotubes completely embedded in oxide. The tubes were embedded in oxide using a selective CVD technique.[12] The silicon dioxide selectively coated the nanotubes where they were in contact with the trench tops, and not where they were suspended over the trenches. To ensure that no oxide was on the suspended portion of the tube, the oxide was etched in 40% NH_4F for 2 min. This solution etched the silicon dioxide film at a rate of 0.4 Å/s, leaving 11 nm of oxide on the trench tops.

For quantitative measurements of slipping events, nanotubes were pushed only far enough for slip to be detected. This allowed measurements of the critical tension needed to cause slip as well as changes in suspended tube length, or slack, after slipping events.

The adhesion of the nanotubes to the silicon dioxide surface was measured using a Digital Instruments Dimension 3100 AFM, in AC mode. The AFM was used to find a nanotube crossing at least one trench, and then centered on one suspended section to be used for pushing. After allowing the microscope to scan for 5−10 min and recentering to reduce $x-y$ drift, the suspended portion of the tube was pushed in the z direction, as diagrammed in Figure 1a and b. In the AFM force versus distance measurements, the amplitude and deflection signals were recorded during the z-axis extension (toward the sample surface) and retraction (away from the sample surface) of the AFM scanner. The amplitude and deflection traces were then used to determine the tension in the suspended nanotube. The spring constant of each individual cantilever was determined using the resonant frequency and the geometry of the cantilever, as described elsewhere.[13] AFM probes from two sources, Veeco Probes and MikroMasch, were used in the measurements.

* Corresponding author. E-mail: davis@byu.edu; tel: (801)422−3238.
† Brigham Young University.
‡ Cornell University.
§ Pomona College.

10.1021/nl060018t CCC: $33.50
Published on Web 04/19/2006

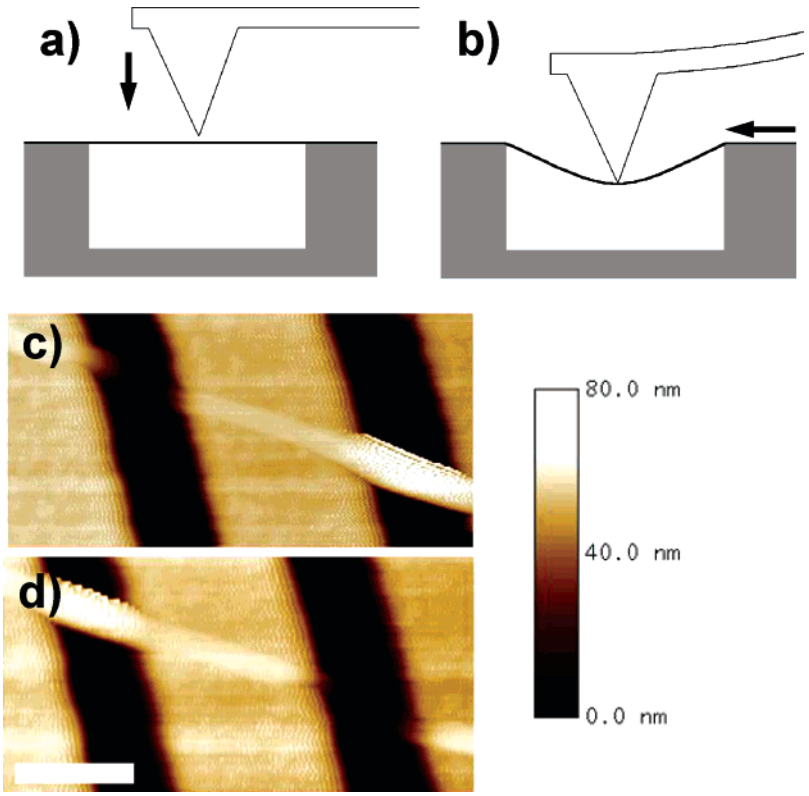

Figure 1. (a) Tip approaching tube for pushing. (b) Tip exerting force on tube until slip occurs across a trench top. (c) AFM image of nanotube crossing two trenches; the left suspended section has been pushed down and stuck to the trench bottom. (d) AFM image of the same tube and trenches after pushing the right suspended section down to the trench bottom; the left section has become suspended again. Scale bars are 250 nm.

The Veeco probes (model no. NP-S) have a nominal tip radius of curvature of 20 nm; we measured the spring constant of each of the Veeco probes to be 0.24 N/m. The MikroMasch probes (model no. NSC12/ALBS/3) have a nominal tip radius of curvature of 10 nm; we measured the spring constant of the MikroMasch probes to be 0.14 N/m.

Figure 2 is a schematic of the tube pushing process, where z_{PIEZO} is the extension or retraction of the AFM scanner relative to the equilibrium position of the nanotube. L_o is the distance between anchoring points, θ is the angle between the nanotube's location and its equilibrium position, z_{DEFL} is the DC deflection signal due to the bending of the cantilever, and z_{TIP} is the position of the probe tip relative to the nanotube's equilibrium position. The positive z axis is normal to the sample surface, so z_{TIP} is negative while force is being applied to the nanotube.

The amplitude and deflection traces for a push on a nanotube where no slip occurred are shown in Figure 3a and b. On the right side of the amplitude trace we see the free oscillation amplitude of the cantilever as it approaches the tube. When the tip contacts the tube, the amplitude drops suddenly and then rises until the tube's equilibrium position is reached (the tip is level with the trench top). At this point the tip can oscillate almost freely due to slack in the nanotube. The amplitude drops as the tip pushes the nanotube beyond its equilibrium position, dropping to zero when there is no longer slack in the tube. As the tube becomes taut the deflection signal rises as force is applied by the tip to the nanotube. We label this onset of tensioning of the tube z_{ONSET} (Figure 3b). The deflection data agree with the expected curve shape for CNT elastic deformation.[5] The reverse occurs on retraction, that is, the amplitude and deflection traces closely follow the same path as they did on extension. The amplitude peaks line up as the equilibrium position of the nanotube with respect to the tip has not changed. The adhesion force between

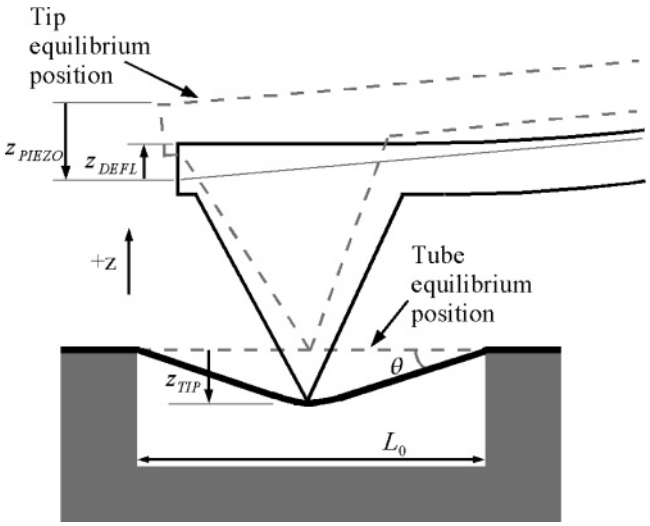

Figure 2. Schematic of tube pushing. The vertical position of the tip is determined relative to the equilibrium position. z_{TIP} is given by $z_{TIP} = z_{PIEZO} + z_{DEFL}$. z_{PIEZO} is also measured relative to the equilibrium position. L_o is the distance between NT anchoring points, and $\theta = \tan^{-1}(2\ z_{TIP}/L_o)$.

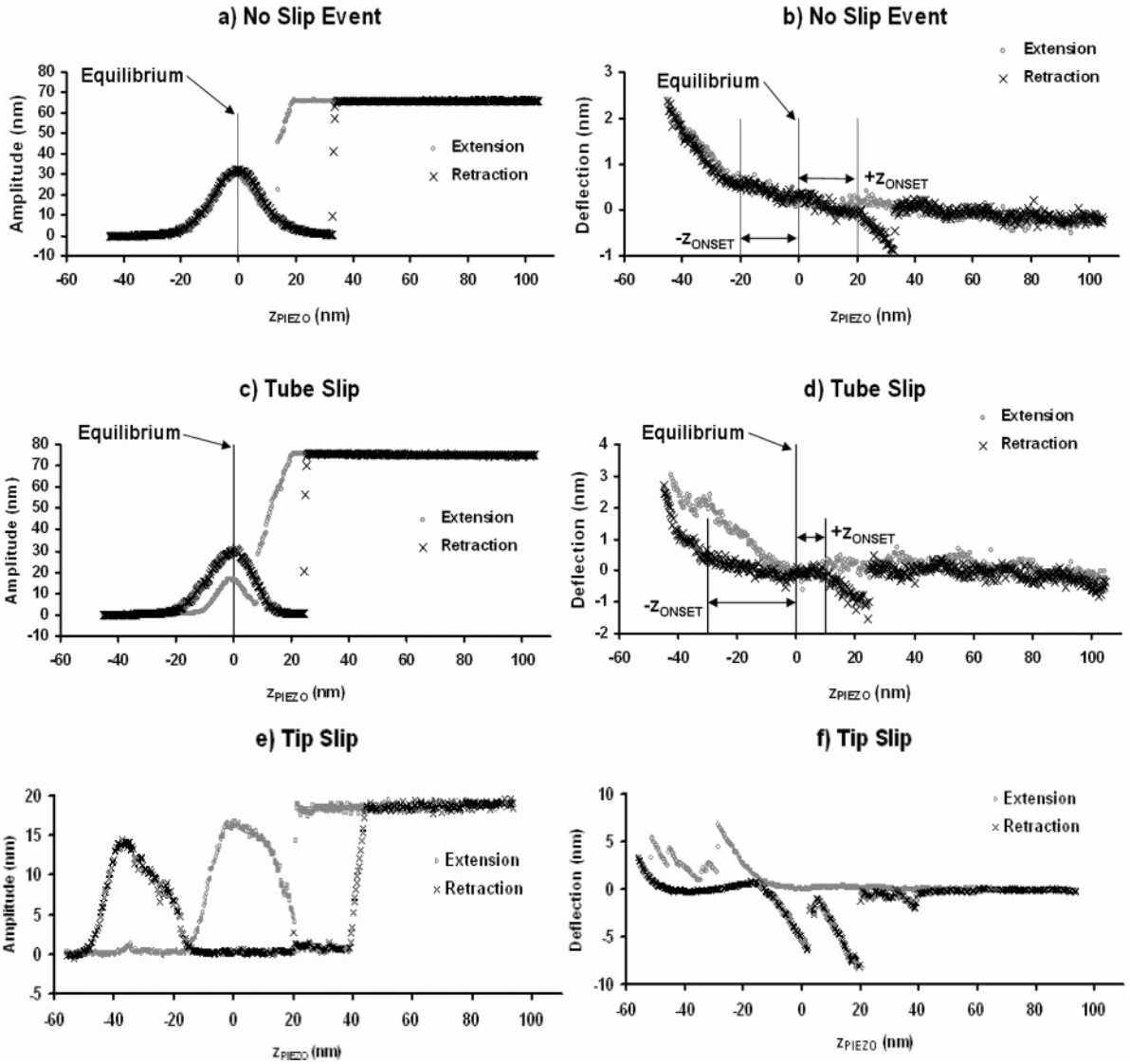

Figure 3. Amplitude and deflection traces for a (a−b) no-slipping event at a maximum tension of 7 nN, (c−d) tube slipping along the trench top at a critical tension of 12 nN, and (e−f) tube sliding up the side of an AFM tip. None of the three cases shown are from data on the same nanotube or using the same AFM cantilever probe.

the tip and the tube is large enough to cause a negative deflection when the tip pulls off the tube during retraction.

When the nanotube slips during an AFM push, the rising deflection signal deviates significantly from that for elastic nanotube deformation; the trace levels off or abruptly drops as slipping occurs. Figure 3d shows deflection leveling off at negative z_{PIEZO} as the tension in the tube is released. On retraction, the region of zero deflection between the two z_{ONSET} points is wider. In this specific case the nanotube relaxes during retraction, giving rise to a $+z_{ONSET}$ that is much shorter than $-z_{ONSET}$. Figure 3f shows abrupt drops in deflection at negative z_{PIEZO} as the tension in the tube is released. In both of these cases the deflection trace on retraction does not follow the deflection trace on extension.

The amplitude signal was particularly important in determining the difference between the tube slipping across the trench tops and the tube slipping up the side of the pyramidal AFM tip. When the tube slips only on the trench top, the amplitude peaks on extension and retraction have the same equilibrium position as seen in Figure 3c. However, on retraction the peak is taller and wider than on extension, indicating increased tube slack. In Figure 3e the apparent location of the tube's equilibrium position has changed, as is seen by an offset between the extension amplitude peak and the retraction amplitude peak; indicating that the tube has slipped on the AFM tip. In this tip-slip event the peak height did not change because the tube slack did not increase. Tip-slip data were discarded in this study.

Tension in the nanotube was calculated using the geometric model[5] shown in Figure 2, with the following equations for vertical force, F, applied by the AFM probe and the tension, T, in the nanotube.

$$F = k_{TIP} z_{DEFL} \tag{1}$$

$$T = \frac{F}{2 \sin \theta} \tag{2}$$

k_{TIP} is the spring constant of the cantilever and z_{DEFL} is the z-deflection signal.

Table 1. Summary of Tube Pushes[a]

tube no.	push no.	T (nN)	dL_{TUBE} (nm)	contact length (nm)	tube diameter (nm)
1	1−1	8	3	228	2
1	1−2	8	3	228	2
2	2−1	7	2	246	2
3	3−1	12	4	140	3
3	3−2	8	3	140	3
4	4−1	7	12	146	3
4	4−2	8	5	146	3
4	4−3	8	4	146	3
4	4−4	8	4	146	3

[a] T is the tension at which slip occurred, and dL_{TUBE} is the change in length of the suspended portion of the tube. The nanotube diameters were measured by AFM.

The increased slack of a nanotube after a slipping event was determined by comparing the deflection versus distance traces before and after a slipping event. The region of zero force seen in Figure 3b, between $+ z_{ONSET}$ and $- z_{ONSET}$, was used to calculate the slack in the tube. The onset of the tensioning of the tube z_{ONSET} was used along with the distance between anchor points, L_o, to calculate the original suspended length of the tube, L_{TUBE}, as follows.

$$L_{TUBE} = 2\sqrt{\left(\frac{L_o}{2}\right)^2 + (z_{ONSET})^2} \qquad (3)$$

The difference in the suspended length of the tube before and after slipping was used to determine the change in the tube's slack.

After increasing slack in a nanotube there is an unstable tension distribution on neighboring trenches, which often relaxes to a more stable tension distribution during imaging. This pulls the slack from the previously pushed nanotube so that it is again taut, as seen in the deflection data from Figure 3d.

We pushed on four different nanotubes, and collected the data given in Table 1. Tube 1 was pushed on from its as-grown position twice, and it relaxed between pushes and during AFM imaging. Tubes 2 and 3 were also pushed on from their as-grown positions, and tube 3 did not relax between pushes. Tube 4 was tensioned by kinking it with the AFM probe on the trench top one trench period away, as seen in Figure 4a. After pushing, the kink had been straightened (Figure 4b) by the sliding of 23 nm of nanotube, found by measuring AFM images of the tube before and after. After measuring the left suspended section's length by analyzing the deflection traces, we found that it had increased by 12 nm. This indicates that the two suspended sections of nanotube shared the extra 23 nm of tube length equally. Tube 4 was again tensioned by AFM probe manipulation, this time on a more distant trench. The next three pushes were done in succession.

With the exception of the initial push on tube 3, all of the tubes slid at 7−8 nN of applied tension. They also all gained 2−5 nm of slack in each push, with the exception of the initial push on tube 4 where the tube had been preloaded with tension by kinking. For pushes where no slip occurred, the maximum tension in the nanotube often came close to but never exceeded the critical tension where slip occurred. For each slip reported here, there were two to four pushes where no slip occurred, each being less than the critical tension. The amount of tension required to cause slip did not vary between contact lengths of 140 and 246 nm. Other authors have suggested that the adhesion between CNTs and surfaces cannot be described using a simple macroscopic friction or force per unit length model;[14,15] our results support this across the narrow range of contact lengths we investigated.

Our finding that adhesion force is independent of contact length may be attributed to nanotube stretching. Because the nanotube is more compliant than the substrate, it is likely that slipping first occurs close to the edge of the trenchtop.

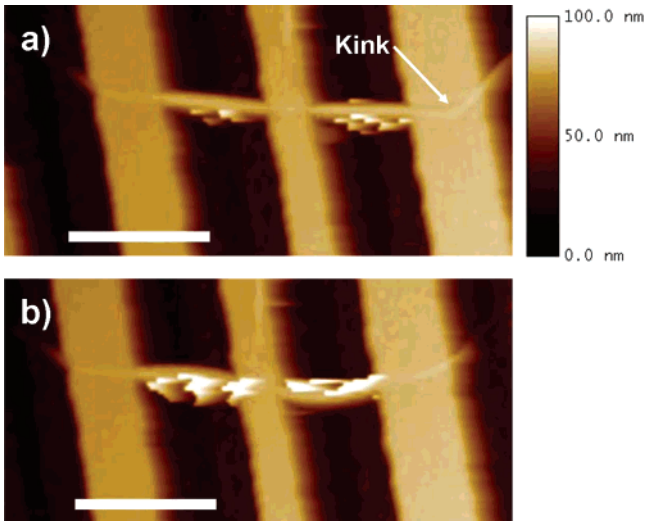

Figure 4. (a) Kinked tube before pushing on the left suspended section. (b) After pushing the left section, the extra length from the kink is in the suspended sections of the tube. Scale bars are 500 nm.

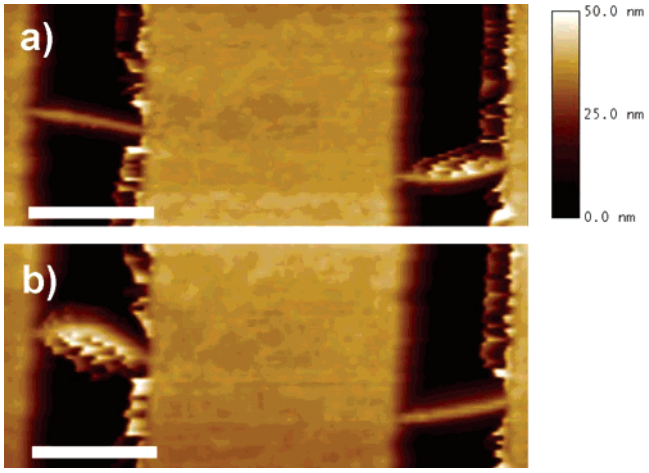

Figure 5. (a) The nanotube is buried on the trench tops by oxide but not coated where it is suspended. The right section has significant slack. (b) After pushing on the left section, the right section is tight and the left section is slack. Slip occurred through the oxide. The scale bar is 200 nm.

For the tensions used in this study, the suspended section of a nanotube is stretched up to 10%. Sections of nanotube that are in contact with the trenchtop will experience less strain. How quickly the strain decreases away from the edge of the trench depends on the difference in compliance between the SiO_2 substrate and the nanotube. For the small-diameter nanotubes used is this study, it is likely that the length scale for the decay of strain (and therefore static friction force) is smaller than our narrowest trenchtops.

After selectively embedding the tubes in oxide and etching back any extemporaneous oxide coating the suspended tube sections over the trenches, we made another pushing measurement. The tube is shown in Figure 5a, which initially had the left section tight and the right section loose. We pushed on the left section until slip occurred at an applied tension of 10 nN. This was slightly higher than the slipping tension of the tubes measured on bare silicon dioxide. Figure 4b shows the tube after pushing. The left section was slack after the push, while the right section had tightened, indicating that slipping occurred through the oxide.

We have shown a method to both cause and measure slip of a nanotube across a silicon dioxide surface. By analyzing amplitude signals and deflection signals during pushing, we have measured critical tension for slip and changes in slack. We find that 7−8 nN of applied tension causes slip along the silicon dioxide, while an embedded tube resists 10 nN of applied tension before slipping through the selectively deposited oxide. The critical tension for causing slip did not depend on the contact length of the tube and surface over the narrow range of contact lengths we investigated (140−246 nm). This suggests that a simple force per unit length friction model is insufficient for describing nanotube adhesion to a silicon dioxide surface.

Acknowledgment. This work was supported by the National Science Foundation Center for Nanoscale Systems at Cornell University. We thank Markus Brink for help with atomic force microscope probe calibration and David Allred and Matthew Linford for useful discussions.

References

(1) Hafner, J.; Cheung, C.-L.; Oosterkamp, T.; Lieber, C. *J. Phys. Chem. B* **2001**, *105*, 743.
(2) Cheung, C.-L.; Hafner, J.; Odom, T.; Kim, K.; Lieber, C. *Appl. Phys. Lett.* **2000**, *76*, 3136.
(3) Wade, L.; Shapiro, I.; Ma, Z.; Quake, S.; Collier, C. *Nano Lett.* **2004**, *4*, 725.
(4) Williams, P.; Papadakis, S.; Patel, A.; Falvo, M.; Washburn, S.; Superfine, R. *Appl. Phys. Lett.* **2003**, *82*, 805.
(5) Minot, E.; Yaish, Y.; Sazonova, V.; Park, J.-Y.; Brink, M.; McEuen, P. *Phys. Rev. Lett.* **2003**, *90*, 156401.
(6) Bachtold, A.; Hadley, P.; Nakanishi, T.; Dekker, C. *Science* **2001**, *294*, 1317.
(7) Hertel, T.; Martel, R.; Avouris, P. *J. Phys. Chem. B* **1998**, *102*, 910.
(8) Falvo, M.; Taylor, R.; Helser, A.; Chi, V.; Brooks, F.; Washburn, S.; Superfine, R. *Nature* **1999**, *397*, 236.
(9) Akita, S.; Nishijima, H.; Kishida, T.; Nakayama, Y. *Jpn. J. Appl. Phys.* **2000**, *39*, 3724.
(10) Vigolo, B.; Pénicaud, A.; Coulon, C.; Sauder, C.; Pailler, R.; Journet, C.; Bernier, P.; Poulin, P. *Science* **2000**, *290*, 1331.
(11) Zhang, M.; Atkinson, K.; Baughman, R. *Science* **2004**, *306*, 1358.
(12) Whittaker, J.; Brink, M.; Husseini, G.; Linford, M.; Davis, R. *Appl. Phys. Lett.* **2003**, *83*, 5307.
(13) Cleveland, J. P.; Manne, S.; Bocek, D.; Hansma, P. K. *Rev. Sci. Instrum.* **1993**, *64*, 403−405.
(14) Decossas, S.; Patrone, L.; Bonnot, A.; Comin, F.; Derivaz, M.; Barski, A.; Chevrier, J. *Surf. Sci.* **2003**, *543*, 57.
(15) Ni, B.; Sinnott, S. *Surf. Sci.* **2001**, *487*, 87.

NL060018T